

**TOMÁŠ CHREBET<sup>1</sup>**  
**KAROL BALOG<sup>2</sup>**  
**JOZEF MARTINKA<sup>3</sup>**  
**IVAN HRUŠOVSKÝ<sup>4</sup>**

<sup>1,2,3,4</sup>Slovak University of Technology  
in Bratislava, Faculty of Materials  
science and Technology in Trnava,  
Institute of Safety and Environmental  
Engineering

<sup>1</sup>tomas.chrebet@stuba.sk

<sup>2</sup>karol.balog@stuba.sk

<sup>3</sup>jozef.martinka@stuba.sk

<sup>4</sup>ivan.hrusovsky@stuba.sk

## MONITORING OF THE CELLULOSE PYROLYSIS IN A MODIFIED ELECTRICALLY HEATED HOT AIR FURNACE

**Abstract:** This paper deals with monitoring of the thermal decomposition of pure cellulose in a modified electrically heated hot air furnace, which allows simultaneous measure of weight loss, released gases (CO, CO<sub>2</sub>, C<sub>x</sub>H<sub>y</sub>, H<sub>2</sub>, NO, NO<sub>2</sub> and O<sub>2</sub>) at a given temperature or a selected heating rate and the selected airflow speed. The measurements were made under isothermal conditions in the temperature range 230-340 °C and air flow at speeds 30, 20, 10, 0 mm.s<sup>-1</sup>.

**Key words:** thermal decomposition, cellulosic materials, evolved gases

### INTRODUCTION

Cellulose, one of the most widely used natural polymers on earth, consists of repeated elements of cellobiose. Cellulose is a linear polymer of β-d-glucose in the pyranose form, linked together by 1,4-glycosidic bonds [1, 2]. Cellulose is a major component of wood, and it is released during combustion of the majority of flammable gases [3]. Therefore, we focused on the reaction of cellulose during thermal decomposition. When cellulose is heated in the temperature range 120 - 350 °C, there are at least three primary reactions: thermo-oxidation, dehydration and depolymerization associated with glycosane formation. The parallel course of these reactions significantly affects the results of the process. Thermo-oxidation and dehydration are controlled by diffusion processes taking place mainly in the proportions of amorphous polysaccharides. At the same time, short chains are formed with depolymerization [4]. Fig. 1 shows the degradation scheme and various processes involved in pyrolysis and combustion of cellulose.

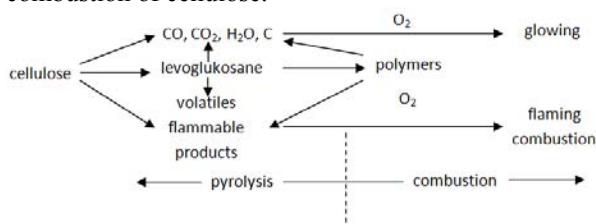


**Figure 1.** Scheme of cellulose degradation and the processes involved in pyrolysis and combustion of cellulose [5]

During thermal straining of different materials, there is exo and endothermic processes associated with weight change, which are characteristic for the tested material. For monitoring these changes, various thermo-analytical methods can be used (thermogravimetry, derivation thermogravimetry, differential thermal analysis, differential scanning calorimetry). During heat straining, there is a development of gaseous

degradation products depending on the temperature of degradation, which can be continuously collected and evaluated [6, 7]. The disadvantage of simple thermo-analytical methods is possibility to monitor only one physical properties using one sample. With the simultaneous method, we can explore more physical properties simultaneously during one measurement using one sample.

We modify the electrically heated hot air furnace in order to perform simultaneous measurement of weight loss, mass lose rate and concentration of released gases (CO, CO<sub>2</sub>, C<sub>x</sub>H<sub>y</sub>, H<sub>2</sub>, NO, NO<sub>2</sub>, O<sub>2</sub>) at a given temperature or a selected rate of heating and the selected airflow speed.

### DESCRIPTION OF TEST EQUIPMENT

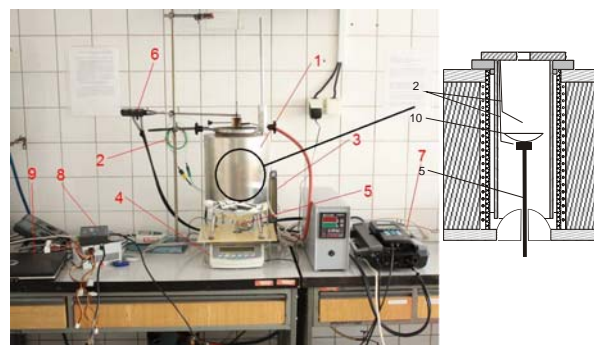


**Figure 2.** Test equipment

The basis of test equipment is electrically heated hot-air furnace according to ISO 871 (the Setchkin furnace) (1). A sample is put in a steel sieve, in order to better monitor the air flow effect in the furnace. Two thermocouples are also placed in the furnace (2), one is about two centimeters above the sample and the second approximately centimeter below the sample. Air is forced to the furnace with air pump; the flow is regulated by flow meter (3). Under the furnace, there is weight (KERN PLT 450-3M) (4). The sieve with the sample in the furnace is linked with weight using a

glass rod (5), which is on both sides flat extended for stability. Above the opening of the flow decomposition products there is a sampling probe (6) of gas analyzer (TESTO 350XL) (7); this analyzer can monitor O<sub>2</sub>, CO, CO<sub>2</sub>, CxHy, H<sub>2</sub>, NO, NO<sub>2</sub> and temperature at the sampling place. Thermocouples, weight and gas analyzer are connected via RS 232 to N-port (8) and it is connected to a computer (9).

### Sample preparation, experiment and recorded values

The sample of pure cellulose was filter paper with density 100g/m<sup>2</sup>, which was cut into squares of approximately 15mm, and the loading of 2g. The sample was evenly distributed in the sample holder (strainer). When dynamic changing of temperature has been applied, the heating rate was 5 °C/min<sup>-1</sup>. In isothermal condition, the furnace has been left tempered during 30 minutes on set temperature, then the sample was inserted into the furnace and the measurement starts. Data from the weight, thermocouples and gas analyzers were recorded every 5 seconds. Samples in which change was not observed were left for three hours in the furnace.

### The course of the experiment

By the initial non-isothermal (dynamic) method, we get an overview of the overall thermal behavior of explored sample for the entire temperature range. However, it is not possible to observe self heating processes, the impact of external factors on this process or to determine critical conditions. For the monitoring of burning, self heating and flameless combustion processes, isothermal conditions are considered to be suitable. Therefore, we focused on finding the lowest temperature at which pyrolysis can be observed at different speeds of air flow around the sample.

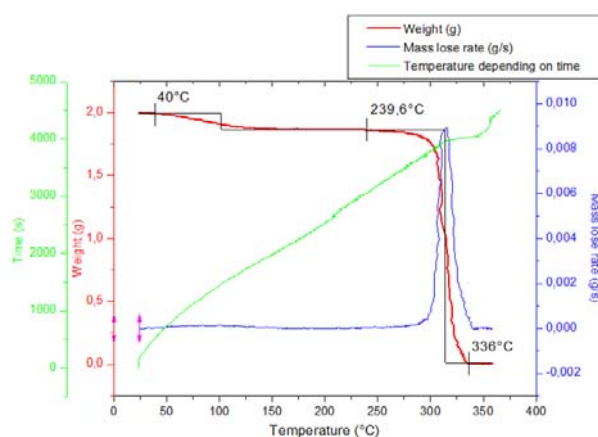


**Figure 3.** TG / DTG record, 2 grams sampe of pure cellulose, heating rate 5°C.min<sup>-1</sup> using sieve and velocity of airflow 25 mm.s<sup>-1</sup>

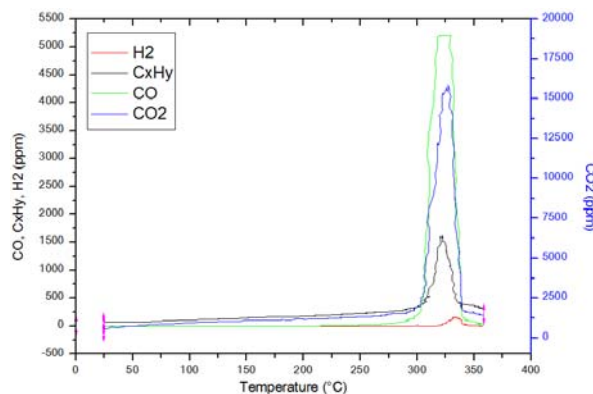


**Figure 4.** Dependence of released gases from temperature, 2 grams sampe of pure cellulose, heating rate 5°C.min<sup>-1</sup> using sieve and velocity of airflow 25 mm.s<sup>-1</sup>

For overall mapping of processes at different temperatures, we chose the highest temperature of 20 °C above the temperature at which the maximum mass lose rate was observed during dynamically changing temperature (Fig. 3, 4), i.e. 340 °C, and further temperature have been 10 °C lower than the previous one. We also monitor the impact of air flow velocity into the reaction zone, we choose airflow speed: 30, 20, 10, 0 mm/s<sup>-1</sup> converted to the appropriate temperature according to the relationship mentioned in the standard [8].

Measurements taken under isothermal conditions enabled us to calculate the activation energy of initiation and propagation phase of degradation of pure cellulose sample by Arrhenius equation (1):

$$k = Z \cdot e^{\frac{-E}{RT}} \quad (1)$$

where Z is the frequency factor, E is the activation energy, R is the gas constant and T is absolute temperature.

### RESULTS OF EXPERIMENTS

With regard to the large amount of measured results, we would like to mention the example graph for pure cellulose at temperature of 340 °C and airflow velocity 30 mm/s<sup>-1</sup>. The graphs are displayed from the top, the time dependence of oxygen concentration in % and average temperature (average temperature between the thermocouple located above the sample and below the sample) in °C, time dependence of hydrogen and hydrocarbon concentration in ppm (parts per million), time dependency of carbon monoxide and carbon dioxide in ppm, the time dependence of the proportion CO<sub>2</sub>, CO, H<sub>2</sub>, CxHy, and time dependency of TG / DTG with marked times of decomposition stages. To draw graphs, we used a trend line in the originlab program marked as Smoothing, method of rendering Savitzky-Golay, polynomial order 1.

**Criteria for evaluation:**

- Time to mass loss rate  $0,0004 \text{ g.s}^{-1}$  in the second stage of decomposition (this value was determined as the lowest mass loss rate which is followed by decomposition of the sample) (Fig. 5 Position 1)
- Duration of pyrolysis (time interval from the mass loss rate  $0,0004 \text{ g.s}^{-1}$  to the end of the second phase of decomposition, we did not counting the glowing interval) (Fig. 5 Position 2)
- Time to Bamford critery (mass loss rate of  $0,005 \text{ g.s}^{-1}$ , which are conditions for the ignition) (Fig. 5 Position 3)
- Concentration of  $\text{CO}$ ,  $\text{CO}_2$  and the ratio of  $\text{CO}/\text{CO}_2$  when was Bamford critery achieved (Fig. 5 Position 4, 5)
- Time to maximum concentration of  $\text{CO}$  (Fig. 5 Position 6)
- Time to maximum concentration of  $\text{CO}_2$  (Fig. 5 Position 7)
- With regard to that there were problems with the initial concentration of  $\text{C}_x\text{H}_y$ , and concentration of  $\text{H}_2$  is count from measured values of  $\text{C}_x\text{H}_y$  we did not deal with these gases any more in the graph on fig. 5 are shown only for illustration.

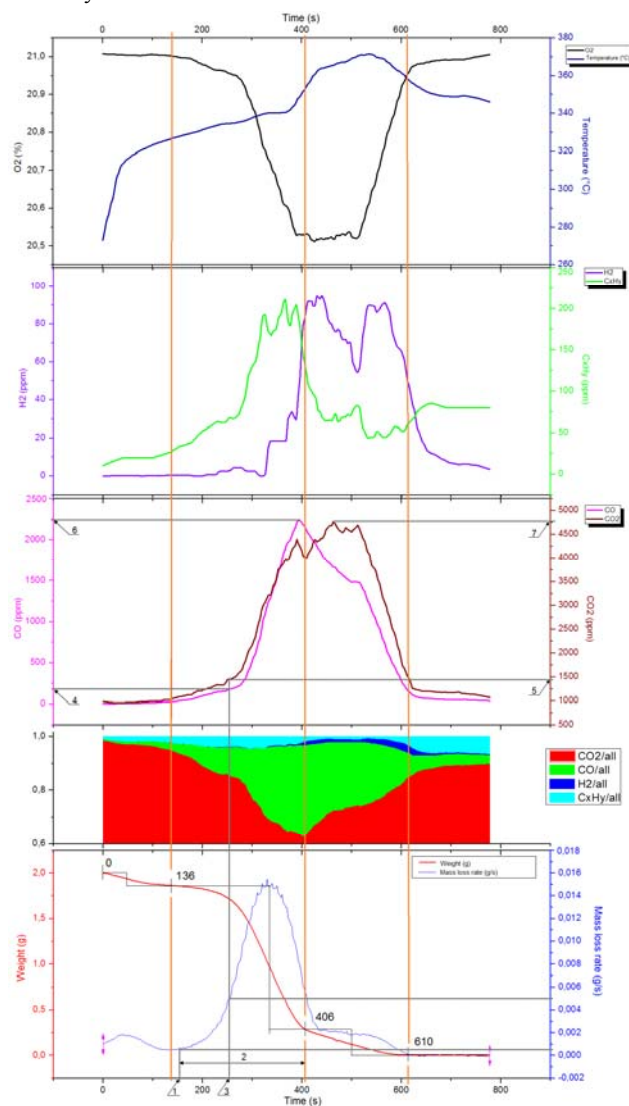


**Figure 5.** Time dependence at  $340^\circ \text{C}$  and a airflow velocity of  $30 \text{ mm.s}^{-1}$ . Graphs are showing from the top: the time dependence of oxygen concentration in % and average temperature in  $^\circ \text{C}$  oven, the time dependence of hydrogen

and hydrocarbon concentration in ppm, time dependency of carbon monoxide and carbon dioxide in ppm, the time dependence of the proportion of  $\text{CO}_2$ ,  $\text{CO}$ ,  $\text{H}_2$ ,  $\text{C}_x\text{H}_y$  and time dependence of weight loss in g and mass loss rate in  $\text{g.s}^{-1}$ .

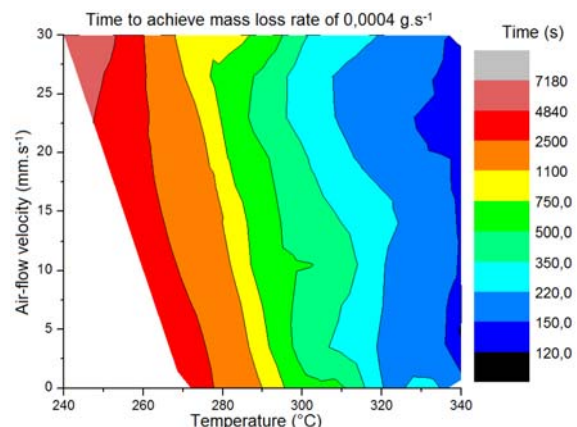


**Figure 6.** Time to achieve mass loss rate of  $0,0004 \text{ g.s}^{-1}$  in dependence on temperature and airflow velocity

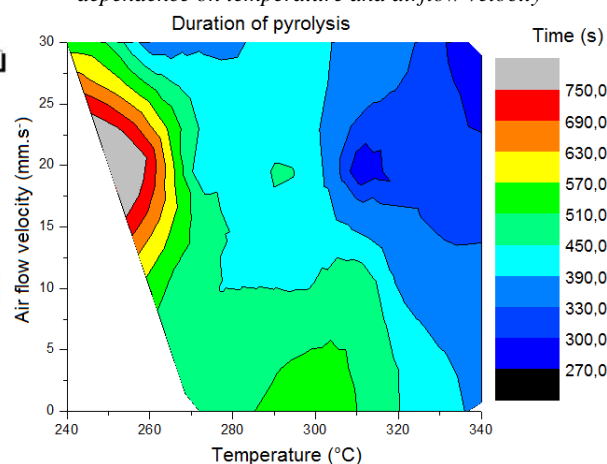


**Figure 7.** Duration of pyrolysis in dependence on temperature and airflow velocity

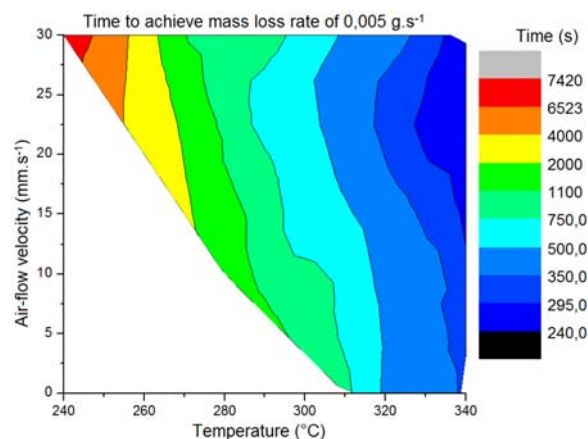


**Figure 8.** Time to achieve mass loss rate of  $0,005 \text{ g.s}^{-1}$  in dependence on temperature and airflow velocity



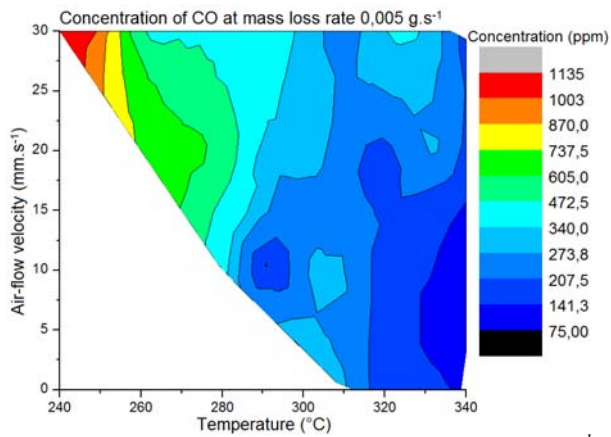


Figure 9. Concentration of CO at mass loss rate  $0,005 \text{ g.s}^{-1}$  in dependence on temperature and airflow velocity

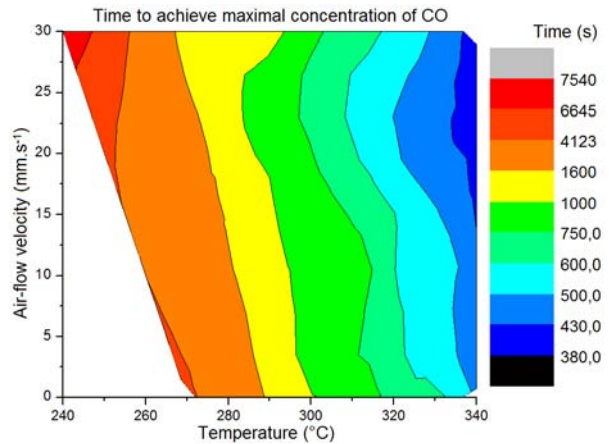


Figure 12. Time to achieve maximal concentration of CO in dependence on temperature and airflow velocity

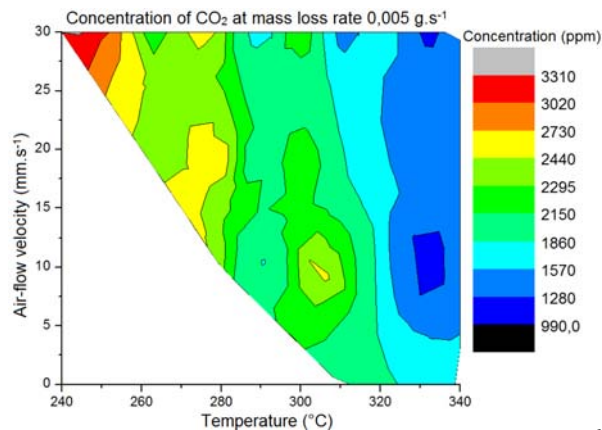


Figure 10. Concentration of  $\text{CO}_2$  at mass loss rate  $0,005 \text{ g.s}^{-1}$  in dependence on temperature and airflow velocity

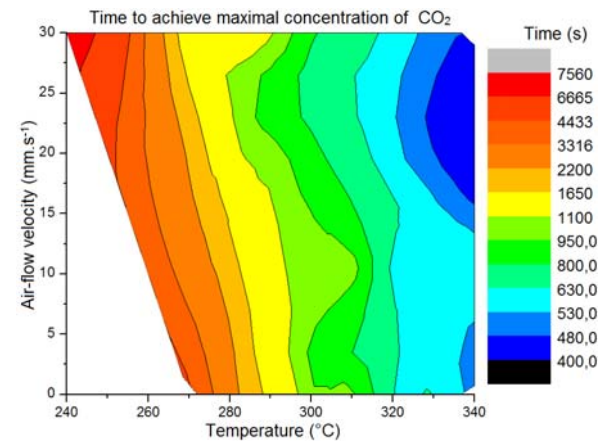


Figure 13. Time to achieve maximal concentration of  $\text{CO}_2$  in dependence on temperature and airflow velocity

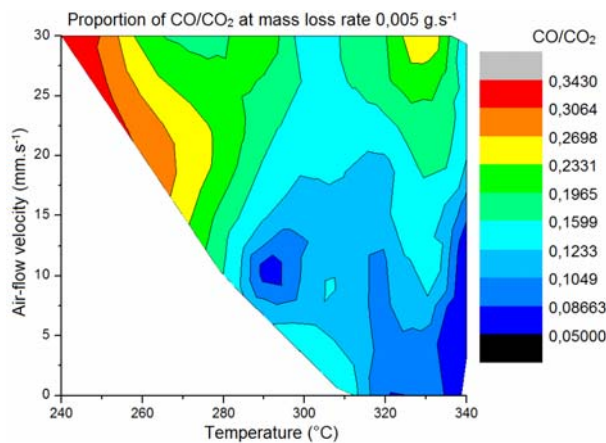


Figure 11. Proportion of  $\text{CO}/\text{CO}_2$  at mass loss rate  $0,005 \text{ g.s}^{-1}$  in dependence on temperature and airflow velocity

Table 1. Time to achieve mass loss rate of  $0,0004 \text{ g.s}^{-1}$  depending on temperature and airflow velocity

Air flow velocity [mm.s <sup>-1</sup> ]	Time [s] to achieve mass loss rate of $0,0004 \text{ g.s}^{-1}$										
	Temperature [°C]										
	240	250	260	270	280	290	300	310	320	330	340
30	7180	5790	2520	895	895	655	370	270	215	170	132
20	X	X	2665	1715	765	520	365	235	180	145	146
10	X	X	X	2350	1295	605	515	445	210	210	144
0	X	X	X	4285	2010	1105	550	540	220	245	166

**Table 2.** Duration of pyrolysis in dependence on temperature and airflow velocity

Air flow velocity [mm.s <sup>-1</sup> ]	Duration of pyrolysis [s]										
	Temperature [°C]										
	240	250	260	270	280	290	300	310	320	330	340
30	540	510	350	380	375	630	410	360	345	305	274
20	X	X	750	445	410	455	420	270	325	305	310
10	X	X	X	460	450	450	645	725	380	345	350
0	X	X	X	470	495	525	560	510	450	430	362

**Table 3.** Time to achieve mass loss rate of 0,005 g.s<sup>-1</sup> in dependence on temperature and airflow velocity

Air flow velocity [mm.s <sup>-1</sup> ]	Time [s] to achieve mass loss rate of 0,005 g.s <sup>-1</sup>										
	Temperature [°C]										
	240	250	260	270	280	290	300	310	320	330	340
30	7415	6020	2690	1105	1105	895	630	480	395	325	252
20	X	X	X	1950	1015	775	615	435	345	285	284
10	X	X	X	X	1590	880	800	700	405	385	304
0	X	X	X	X	X	X	X	825	455	475	310

**Table 4.** Concentration of CO at mass loss rate 0,005 g.s<sup>-1</sup> in dependence on temperature and airflow velocity

Air flow velocity [mm.s <sup>-1</sup> ]	Concentration of CO [ppm] at mass loss rate 0,005 g.s <sup>-1</sup>										
	Temperature [°C]										
	240	250	260	270	280	300	310	320	330	340	
30	1134,57	981,762	482,095	453,905	453,905	327,333	238,047	342,429	333,429	175,524	
20	X	X	X	619,476	600	307,714	249,952	162,476	292,19	190,333	
10	X	X	X	X	378,667	267,238	304,714	153,905	158,619	75,5714	
0	X	X	X	X	X	X	286,667	169	159	127,095	

**Table 5.** Concentration of CO<sub>2</sub> at mass loss rate 0,005 g.s<sup>-1</sup> in dependence on temperature and airflow velocity

Air flow velocity [mm.s <sup>-1</sup> ]	Concentration of CO <sub>2</sub> [ppm] at mass loss rate 0,005 g.s <sup>-1</sup>										
	Temperature [°C]										
	240	250	260	270	280	300	310	320	330	340	
30	3309,52	3214,29	2242,86	2414,29	2414,29	2380,95	1433,33	1814,29	1214,29	1447,62	
20	X	X	X	2342,86	2680,95	2404,76	1790,48	1580,95	1519,05	1514,29	
10	X	X	X	X	2357,14	2395,24	2419,05	1804,76	990,476	1504,76	
0	X	X	X	X	X	X	2023,81	1938,1	1761,9	1685,71	

**Table 6.** Proportion of CO/CO<sub>2</sub> at mass loss rate 0,005 g.s<sup>-1</sup> in dependence on temperature and airflow velocity

Air flow velocity [mm.s <sup>-1</sup> ]	Proportion of CO/CO <sub>2</sub> at mass loss rate 0,005 g.s <sup>-1</sup>										
	Temperature [°C]										
	240	250	260	270	280	300	310	320	330	340	
30	0,34282	0,30544	0,21495	0,18801	0,18801	0,13748	0,16608	0,18874	0,27459	0,12125	
20	X	X	X	0,26441	0,2238	0,12796	0,1396	0,10277	0,19235	0,12569	
10	X	X	X	X	0,16065	0,11157	0,12596	0,08528	0,16014	0,05022	
0	X	X	X	X	X	X	0,14165	0,0872	0,09024	0,0754	

**Table 7.** Time to achieve maximal concentration of CO in dependence on temperature and airflow velocity

Air flow velocity [mm.s <sup>-1</sup> ]	Time [s] to achieve maximal concentration of CO										
	Temperature [°C]										
	240	250	260	270	280	300	310	320	330	340	
30	7525	6130	2830	1305	1305	795	675	570	490	392	
20	X	X	3020	2140	1165	755	610	510	440	422	
10	X	X	X	2790	1715	960	900	585	560	442	
0	X	X	X	4695	2475	1010	975	650	625	484	

**Table 8.** Maximal concentration of CO in dependence on temperature and airflow velocity

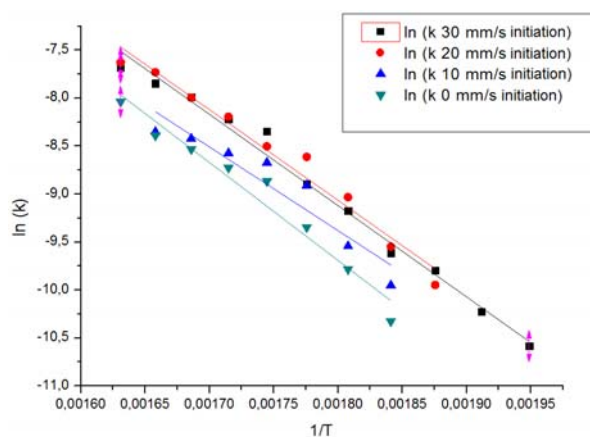
Air flow velocity [mm.s <sup>-1</sup> ]	Maximal concentration of CO [ppm]										
	Temperature [°C]										
	240	250	260	270	280	300	310	320	330	340	
30	1784,86	1619,29	1118,81	1991,95	1991,95	2175,38	1423,67	2000,1	2304,86	2234,71	
20	X	X	955,905	1093,52	1582,57	1511,86	1414,19	1595,67	1973,05	1668,19	
10	X	X	X	553,286	771,333	1118,43	1274,43	1189	1154,24	566,143	
0	X	X	X	140,762	373,905	576,143	577,524	616,381	565,19	613,286	

**Table 9.** Time to achieve maximal concentration of CO<sub>2</sub> in dependence on temperature and airflow velocity

Air flow velocity [mm.s <sup>-1</sup> ]	Time [s] to achieve maximal concentration of CO <sub>2</sub>									
	Temperature [°C]									
	240	250	260	270	280	300	310	320	330	340
30	7550	6150	3030	1310	1310	820	715	585	505	462
20	X	X	3190	2110	1185	845	700	550	480	414
10	X	X	X	2865	1875	1040	1025	580	575	592
0	X	X	X	4690	2475	965	995	630	640	482

**Table 10.** Maximal concentration of CO<sub>2</sub> in dependence on temperature and airflow velocity

Air flow velocity [mm.s <sup>-1</sup> ]	Maximal concentration of CO <sub>2</sub> [ppm]									
	Temperature [°C]									
	240	250	260	270	280	300	310	320	330	340
30	4980,95	4747,62	3261,9	5690,48	5690,48	5342,86	3861,9	4557,14	4523,81	4747,62
20	X	X	3542,86	3123,81	4219,05	448,714	4223,81	4214,29	3957,14	3814,29
10	X	X	X	2714,29	3009,52	3809,52	4352,38	3404,76	2319,05	2476,19
0	X	X	X	1723,81	228,952	2952	2542,86	2604,76	2342,86	2590,48

**Figure 14.** Dependence  $\ln(k)$  vs  $1/T$  for determination of activation energy of initiation phase of degradation for air flow 30, 20, 10, 0 mm.s<sup>-1</sup>**Table 11.** Activation energy of initiation and propagation phase of degradation of pure cellulose

Air flow velocity [mm.s <sup>-1</sup> ]	$E_{\text{initiation}}$ [kJ/mol]
30	79,1
20	78,58
10	72,5
0	84,8

## RESULTS AND DISCUSSION

Degradation of pure cellulose samples pass of at all temperatures and air flow velocity equally in three stages, as it can be seen in Fig.5. In the first stage, there was dehydration from weight loss of approximately 7,1 % and in the second stage, there was the main decomposition where weight loss was 75 % in the third stage there was the glowing and weight loss 16,3%, the resistant remaining after decomposition was about 1,3 % of original weight.

Achieving mass loss rate 0,0004 g/s<sup>-1</sup> characterizes the creation of conditions for thermal decomposition, in Fig. 6 and Tab. 1 times to achieve this mass loss rate have been shown. With decreasing temperature, the longer time is needed to reach this mass loss rate. At air

flow velocity of 30 mm/s<sup>-1</sup>, the decomposition was not observed at temperature 230°C at air flow velocity of 20 mm/s<sup>-1</sup> at 250°C, at air flow velocity of 10 mm/s<sup>-1</sup> and 0 mm/s<sup>-1</sup> at 260°C.

Since the mass loss rate achieves 0,0004 g/s<sup>-1</sup> the greatest weight loss has occurred. Duration of this phase is shown in fig.7 and tab.2, and the influence of air flow can be seen. With the decreasing velocity of air flow at the same temperatures, the duration of this decomposition phase increases.

Fig.8 and tab.3 show time for achieving Bamford criterion, thus creating conditions for the ignition of the volatiles flammable gases by external source. For velocity of air flow 30 mm/s<sup>-1</sup>, a critical temperature is 240°C; for 20 mm/s<sup>-1</sup>, a critical temperature is 270°C; for 10 mm/s<sup>-1</sup>, a critical temperature is 280°C, and when the air flow was not used sufficiently rapid decomposition did not occur below 310°C. Below these temperatures, the samples did not decompose quickly enough.

Concentrations of released CO, CO<sub>2</sub> Fig. 9.10, when was Bamford criterion reached decreasing with increasing temperature. With decreasing velocity of air flow, enough oxygen has not been received during the reaction zone, which reflected the formation of large amounts of CO compared to CO<sub>2</sub> which can be seen on proportion of CO/CO<sub>2</sub> fig.11 tab. 6.

The largest increase of concentrations was observed in case of carbon monoxide, the percentage representation of concentration to the concentration of all measured gases increased about 35 % - Fig.5 (406 s).

The concentration of CO reached a maximum at the end of the main degradation. Maximum concentrations are achieved in Table 12, and the times when the maximal concentrations were achieved are shown in Table 7. Fig. 12 represents the time to reach maximal concentration of CO is increased with decreasing temperature, and air flow velocity had a little effect.

The concentration of CO<sub>2</sub> reached a peak in the early stages of glowing. The table 10 shows maximum concentrations; Table 9 shows times when the

maximum concentrations were achieved. Fig.13 shows the time of peak concentration of CO<sub>2</sub> with increasing temperature decreasing and air-flow had as well as with CO, only a minor impact.

## CONCLUSION

We made measurements in which we monitored the impact of temperature and velocity of air flow around the sample to pure cellulose degradation. At dynamically changing temperature, we found that the highest weight loss occurred at the temperature range between 280°C and 340°C, which coincides well with the TG record of pure cellulose made by standard method. In isothermal conditions, we found that the velocity of airflow 30 mm/s<sup>-1</sup> created conditions for ignition even at 240°C but only after 7415 seconds. With decreasing velocity of the airflow, the temperature is rising. A modified furnace can be used for detailed exploration of the degradation processes of other materials.

## REFERENCES

- [1] Suuberg E. M.: Behavior of Charring Materials in Simulated Fire Environments NIST, 1994 dostupné na: <http://fire.nist.gov/bfrlpubs/fire94/PDF/f94009.pdf>
- [2] Kačík, F., Kačíková, D., Jablonský, M., Katusčák, S.: Cellulose degradation in newsprint paper ageing, Polymer Degradation and Stability 94 (2009) 1509–1514 dostupné na: [www.sciencedirect.com](http://www.sciencedirect.com)
- [3] Shaw, J.,R.: Fire-retardant and flame-resistant treatments of cellulosic materials, Fire Protection Handbook, National Fire Protection Association, Quincy, 2003, str. 8-47, ISBN: 0-87765-474-3
- [4] Kačík, F., Marková, I. Thermal decomposition of main wood components: part II: cellulose In: Wood, roč. 55, 2000, č.6, ISSN 0012-6144
- [5] Butt, D. Thermochemical processing of agroforestry biomass for furans, phenols, cellulose and essential oils.

Rural Industries Research and Development Corporation. Publication, 2006, No. 06/121, 169 p. ISBN 1-74151-384-7

- [6] Růžička M.,Bursíková P.,Dvořák O., Using STA/MS technique in detection of plastics thermal degradation products, Požární ochrana 2008, Sborník přednášek, ISBN 978-80-7385-040-1
- [7] Thermal analysis – theory, accesible in: [http://www.vscht.cz/met/stranky/vyuka/labcv/labor/fm\\_terminicka\\_analyza/teorie.htm](http://www.vscht.cz/met/stranky/vyuka/labcv/labor/fm_terminicka_analyza/teorie.htm)
- [8] ISO 871: 2010 Plastics – Determination of ignition temperature using a hot-air furnace

## ACKNOWLEDGEMENTS

This paper is part of the Project:  
Center for research and application progressive methods in treatment process of metallic and nonmetallic materials, ITMS 26220120048, project implementation: 01/2010 - 12/2011.

## BIBLIOGRAPHY

**Tomáš Chrebet** was born in Bojnice, Slovakia, in 1984. He received the diploma in Non-metallic materials and the PhD. degree in Integrated Safety from the Slovak University of Technology, Faculty of Materials Science and Technology in Trnava.



His main areas of research include mass loss rate, ignitability and flamability etc.

He is currently working as a research worker at Institute of Safety and Environmental Engineering, Faculty of Materials Science and Technology in Trnava.